ChemComm

COMMUNICATION

View Article Online
View Journal | View Issue

Cite this: *Chem. Commun.*, 2016, 52, 10147

Received 19th May 2016,
Accepted 19th July 2016

DOI: 10.1039/c6cc04212k

www.rsc.org/chemcomm



# Smooth and solid $WS_2$ submicrospheres grown by a new laser fragmentation and reshaping process with enhanced tribological properties†

Ting Luo,[a] Ping Wang,[a] Zhiwen Qiu,[a] Shuhua Yang,[a] Haibo Zeng[b] and Bingqiang Cao*[a]

**Smooth and solid $WS_2$ submicrospheres were prepared by a laser irradiation induced fragmentation and morphological reshaping process using bulk-slice $WS_2$ particles as targets in solution. Such submicrospheres as additives in paraffin liquid show remarkably enhanced friction reduction and anti-wear properties in comparison with raw $WS_2$ slices.**

Since the rise of graphene, atomically thin layered materials have been widely and intensively studied.[1] Such new atomically thin transition metal dichalcogenide ($MX_2$; M = Mo, W, Nb, Re; X = S, Se, Te) layers attract much attention from the standpoints of both fundamental physics and applications due to their unique electronic, optical, and mechanical properties.[2] Among them, tungsten disulphide ($WS_2$) has a typical layered structure in the form of a W atomic layer sandwiched between two hexagonal chalcogen atomic layers.[3] Since the discovery of inorganic-fullerene (IF) like $WS_2$ with few closed-layer structures, its application in mechanical areas like tribology is highly desirable as solid lubricants or lubricant additives.[4] As one-third of the total mechanical energy is wasted in friction, friction and wear has been widely recognized as one primary factor in energy loss and failure for all types of mechanical systems such as gears and engine components.[5]

Spherical IF-$WS_2$ powders as additives in lubricant oil usually possess lubricating properties superior to those of 2H-$WS_2$ slices under a wide range of operating conditions.[4c,6] Closed-layer IF-$WS_2$ structures without rim-edge surfaces and active dangling bonds have better chemical stability at high temperature and allow the particles to roll rather than slide during friction. Up to now, much effort has been devoted to the synthesis of novel IF-structures and various methods have been reported, such as the solid–gas reaction between $WO_3$ and $H_2S/H_2$, arc discharge in high-pressure nitrogen, sonoelectrochemical deposition from thiomolybdate solution, and decomposition of metal trisulfides.[7] Among these methods, so far, the most effective synthesis strategy is the solid–gas reaction, which requires high temperature, expensive or toxic high-purity gas, and harsh conditions but still gives low yields. Moreover, the vapour phase produced $WS_2$ particles are of low spherical degree and exhibit a limited effect as lubricant additives.[4a,8]

Laser ablation in liquid (LAL) can create extreme nonequilibrium conditions in nature such as ultrahigh temperature[9] and ultrahigh pressure[10] in few nanoseconds. Yang *et al.* explored this simple but effective route systematically to grow novel nanoparticles, *e.g.*, metastable hexagonal diamonds, silicon nanospheres, and carbon nanocubes.[11] Laser irradiation in liquid (LIL) that usually adopts similar LAL conditions but low laser energy can lead to the reshaping of target particles, which is similar to the laser surface patterning of metals.[12] Previously, we have synthesized ZnO,[13a] SiC,[9b] and FeO[13b] nanoparticles using the LAL method, and $Fe_3O_4$,[13c] CuO, $TiO_2$[9a] and $ZnO/Al_2O_3$[13d] nano/micro-spheres using the LIL method and explored their physical and mechanical properties.

In this communication, we demonstrate a new laser assisted growth strategy for solid $WS_2$ submicrometer spheres with smooth surfaces including the laser induced fragmentation and reshaping (LFR) process, in which bulk-slice $WS_2$ powders are chosen as new targets for laser irradiation in liquid. The fragmentation of bulk-slice $WS_2$ and reshaping of nearly closed sphere cage-like structures were achieved under simple one-step laser irradiation in an ambient environment. The tribological performance of $WS_2$ submicrospheres as additives in paraffin liquid (PL) is evaluated, showing significantly better friction reduction and anti-wear properties when compared with raw $WS_2$ slices. This is a high-yield and cost-effective method to produce smooth and solid $WS_2$ submicrospheres with great potential for industrial production of lubricating oil additives showing a prominent energy-saving effect.

As schematically demonstrated in Fig. 1a, the whole growth process can be conducted under one-step laser irradiation, which experiences typical extreme non-equilibrium conditions in nature

[a] *Materials Research Center for Energy and Photoelectrochemical Conversion, School of Material Science and Engineering, University of Jinan, Jinan 250022, Shandong, China. E-mail: mse_caobq@ujn.edu.cn; Fax: +86-0531-89736292; Tel: +86-0531-89736292*

[b] *School of Material Science and Engineering, Nanjing University of Science and Technology, Nanjing 250022, Jiangsu, China*

† Electronic supplementary information (ESI) available: SEM, XRD, XPS and tribological property test data. See DOI: 10.1039/c6cc04212k

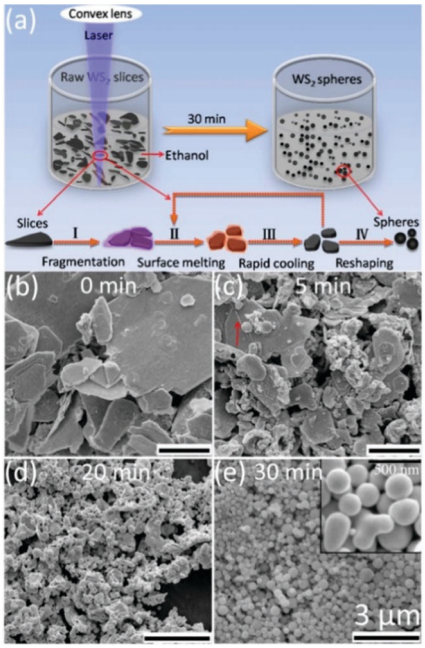


Fig. 1 (a) Schematic illustration of the growth of smooth and solid $WS_2$ submicrospheres using bulk $WS_2$ slices as targets in ethanol by a laser induced fragmentation and reshaping process. (b) SEM image of raw $WS_2$ slices. (c–e) SEM images of the $WS_2$ particles after laser irradiation with a fluence of 700 mJ pulse$^{-1}$ cm$^{-2}$ for different times. Inset in (e): corresponding magnified image.

like high temperature ($>10^4$ K), high pressure (1 Gpa), and high kinetic energy ($>1$ eV).[9b] The particle morphology change from slices to spheres is supposed to be finished by two steps. When one laser beam first strikes the raw $WS_2$ slices, a high pressure is applied onto the laser spot–material interface instantly. Under such a wallop, big $WS_2$ slices explode into smaller fragments (process I in Fig. 1a). After the fragmentation process, more $WS_2$ particles with irregular shapes are produced in the solution. Such particles have high surface area per mass (of the order of 50–300 m$^2$ g$^{-1}$) and high surface energy concentrated in the surface layers,[13c] which is proportional to the surface area and can be released by minimizing the surface area. Continuing pulsed laser irradiation can induce heating and cause melting of the $WS_2$ particle surfaces. Therefore, irregular particles change to spheres gradually with surface energy release, as the spherical structure has the smallest surface area among all surfaces enclosing a given volume (Fig. 1a), as we previously demonstrated.[9a,13c] Meanwhile, dangling W and S bonds at layered edges *via* collisions under laser excitation can rearrange to attain the most stable state. Rapid quenching in liquid within 25 ns upon pulsed heating is helpful to inhibit the reorientation of surface atoms on a spherical particle, and, finally the particles retain the overall spherical structure.

This proposed growth process of spherical $WS_2$ particles is well proved by the morphology evolution of $WS_2$ particles with irradiation time under the same laser fluence, as shown in Fig. 1(b–e). We adopted a relatively high laser energy density (700 mJ pulse$^{-1}$ cm$^{-2}$) to melt the particles. So, raw slice-like $WS_2$ particles (Fig. 1b) begin to fall into small pieces only after 5 minute laser irradiation as shown in Fig. 1c. Small cracks emerge on the surface of bulk slices caused by laser fragmentation (indicated by red arrows). Smaller and quasi-spherical particles in Fig. 1d are observed clearly after 20 min irradiation. Longer laser irradiation (*e.g.* 30 min) results in, on one hand, more ideal spherical particles, and, on the other hand, the merging of particles, as shown in Fig. 1e (inset). That is, several particles begin conjugating into bigger ones. Both particle reshaping into spheres and coalescence reduce their surface area and, accordingly, release the surface energy. The morphology evolution of $WS_2$ particles with the same irradiation time but for different laser fluences (300, 500, 700 mJ pulse$^{-1}$ cm$^{-2}$) is presented in Fig. S2 (ESI†). Clearly, a critical laser energy density is needed to smash and melt the particle surface. For $WS_2$, laser pulses under 700 mJ pulse$^{-1}$ cm$^{-2}$ can produce their submicrospheres within 30 min.

This method is different from the traditional pulsed laser ablation in liquid, in which particle formation is due to the condensation of laser ablated plasma plumes.[10a] It is also different to the traditional LIL in that colloidal nanoparticles are irradiated using a pulsed laser with a wavelength ($\lambda$) comparable to the size ($d$) of target materials ($\lambda \approx d$).[9a] This new method combines the traditional laser fragmentation and laser reshaping, and, therefore, it can be denoted as LFR.

A considerable particle-size reduction of $WS_2$ spheres due to laser fragmentation, compared with raw $WS_2$ slices, can be further measured using a laser particle size analyzer, as shown in Fig. S3 (ESI†). The size distribution of $WS_2$ submicrometer spheres is more uniform (100–400 nm), while the raw $WS_2$ slices have a wide size distribution (0.5–13 μm). The composition and phase purity of $WS_2$ particles are investigated by XRD, as shown in Fig. 2a. The XRD patterns of raw commercial $WS_2$ particles and spherical $WS_2$ particles grown by LFR with a laser fluence of 700 mJ pulse$^{-1}$ cm$^{-2}$ exhibit almost the same diffraction characteristics, and the main content is identified as 2H-$WS_2$ (PDF 08-0237). But, a little metal tungsten (PDF 01-1203) is also detected by comparing the XRD peaks with the standard powder diffraction cards. The XRD pattern of spherical $WS_2$

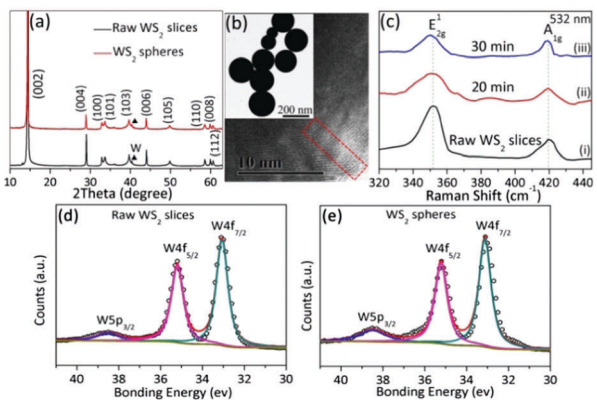


Fig. 2 (a) XRD patterns of raw $WS_2$ slices and $WS_2$ spheres after laser irradiation with a fluence of 700 mJ pulse$^{-1}$ cm$^{-2}$. (b) HRTEM image of smooth $WS_2$ spheres showing some bond combination. (c) Raman spectra of $WS_2$ slices and after 20 and 30 min laser irradiation. (d and e) XPS peaks of tungsten from $WS_2$ raw slices and spheres, respectively.

 

irradiated with a laser fluence of 1000 mJ pulse$^{-1}$ cm$^{-2}$ is much different, and the component percentage of tungsten increased clearly (Fig. S4b, ESI†). It indicates that some reduction chemical reaction(s) occur and change $WS_2$ to W, which is similar to our former report on phase change from $Fe_2O_3$ to $Fe_3O_4$.[13c] After the high-energy LFR process, the number of dangling bonds at the active edges of $WS_2$ slices decreases, where some neighboring bonds combine together, as shown in the HRTEM image of Fig. 2b. Fig. 2c shows the Raman spectra of different $WS_2$ particles and the most intense feature peaks correspond to the $E^1_{2g}$ and $A_{1g}$ modes, which are the atomic displacements for the in-plane phonon mode and the out-of-plane phonon mode, respectively. The $E^1_{2g}$ phonon mode exhibits very subtle redshifts and the relative intensity ratio $I_{E^1_{2g}}/I_{A_{1g}}$ shows significant decreases when the laser irradiation time increases. The XPS results in Fig. 2(d and e) and Fig. S5 (ESI†) show that the relative intensity of $W5p_{3/2}$ in $WS_2$ spheres is higher than that of the raw $WS_2$ slices. All these Raman and XPS changes indicate that partial dangling bonds in such $WS_2$ spheres are closed.[6,14] Moreover, it is worth noting that the smooth surface and perfect sphere shape make the $WS_2$ powder chemically inert. So, it has a lower tendency to stick either to the substrate or to others, and a lower oxidation rate of the surface in the surrounding environment, especially at elevated temperatures during the friction process, which is similar to the chemical stability of IF-$WS_2$.[4a,6]

In light of the spherical shape and smooth surface of $WS_2$ submicrospheres, their tribological properties were measured by adding them in PL in terms of friction coefficient (FC) and wear scar diameter (WSD) using a four-ball tribology tester. Fig. 3 and Fig. S6 (ESI†) show the variation of FC with increasing $WS_2$ concentrations in PL measured at temperatures of 40 °C and 75 °C, respectively. Due to the special 2D layered structure of $WS_2$, it can be seen that the PL samples with $WS_2$ particles, including raw slices (Fig. 3a) and submicrospheres (Fig. 3b), exhibit friction reduction properties in comparison with the pure PL. However, smooth $WS_2$ submicrospheres show dramatically better friction reduction properties than $WS_2$ slices (Fig. 3c), especially at a temperature of 75 °C. The maximum decrease of average FC is about 36.7% for PL with 1.5 wt% $WS_2$ submicrospheres, while the decrease of average FC for $WS_2$ slices is only about 8.9%. When the concentration is less than 2 wt% for slices or 1.5 wt% for submicrospheres, the FCs decrease with increasing $WS_2$ concentration in PL. But, much higher $WS_2$ concentrations lead to an increase of FC.

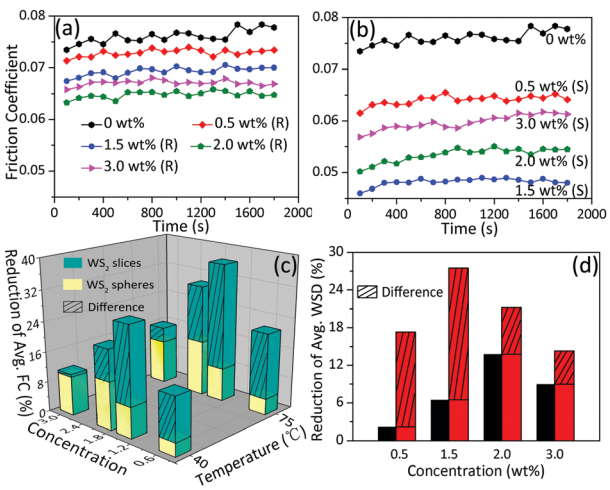


Fig. 3 (a and b) FC variation with time at a temperature of 75 °C for PL with different concentrations of raw $WS_2$ slices (R) and smooth $WS_2$ spheres (S), respectively. (c) Reduction of average FC at temperatures of 40 °C and 75 °C respectively. (d) Reduction of WSD at a temperature of 75 °C.

The anti-wear property is another important characteristic index for lubricating oil. Table S1 (ESI†) compares the average WSDs on the testing balls lubricated by PL with different $WS_2$ concentrations at 75 °C. The influence of $WS_2$ concentration on WSDs is significantly correlated with the change of FCs, as shown in Fig. 3(c and d). The PL sample with 1.5% $WS_2$ spheres presents both the lowest FC and the smallest WSD (decrease by 27.5%). Fig. 4(a and b) show two typical wear scar images of the testing balls lubricated by pure PL and PL with 1.5 wt% $WS_2$ spheres, respectively. The cleaned wear surface after testing in pure PL is very uneven, while the wear furrows from the PL with 1.5 wt% $WS_2$ spheres were small and light. In order to investigate the chemical composition on the wear surface, the energy-dispersive X-ray spectrum (EDX) mapping was carried out, as shown in Fig. 4c. The obvious evidence of W and S element signals is observed, which indicates the formation of a tribofilm with $WS_2$ submicrospheres during the frictional process. The above results confirm that smooth and solid $WS_2$ spheres induced by LFR as additives have an advantage in terms of both friction reduction and anti-wear tribological properties over raw $WS_2$ slices or pure PL.

Up to now, the exact lubricating mechanism of nano/microparticles as lubricant additives for enhanced lubricity is not yet very clear, and it is generally proposed that the tribological role of particles as additives is served as a third body lubrication.[15] During the friction process, layers of $WS_2$ particles are gradually transferred onto the contact surface to form a thicker tribofilm within PL acting as a spacer, preventing metal-to-metal direct contact and providing a reduced sliding friction between the friction pairs as illustrated in process II of Fig. 4d. This can be confirmed by the existence of W and S elements detected by the EDX mapping of the wear surface lubricated by PL with $WS_2$, as shown in Fig. 4c. The enhanced anti-wear performance of lubricating oil containing additives can be explained by the self-repairing mechanism.[13c] Under compressive stress of friction, $WS_2$ particles deposited onto the worn steel surface can fill in the wear scars. This can prevent the enlargement of wear scars and decrease the WSDs.

In addition to the above general lubrication mechanism of ordinary particles, the enhanced tribological performances of such smooth and solid $WS_2$ submicrospheres can also be due to other mechanisms, such as rolling friction and chemical inertness.[12,15] Due to the spherical morphology and absence of partial dangling bonds, $WS_2$ microspheres can work as fullerene-like particles in lubricating oil. When $WS_2$ particles are ideally spherical and smooth, the sliding friction will change to rolling friction using the spheres as molecular bearings as shown in process I of Fig. 4d. Thus, the FCs of PL containing smooth $WS_2$

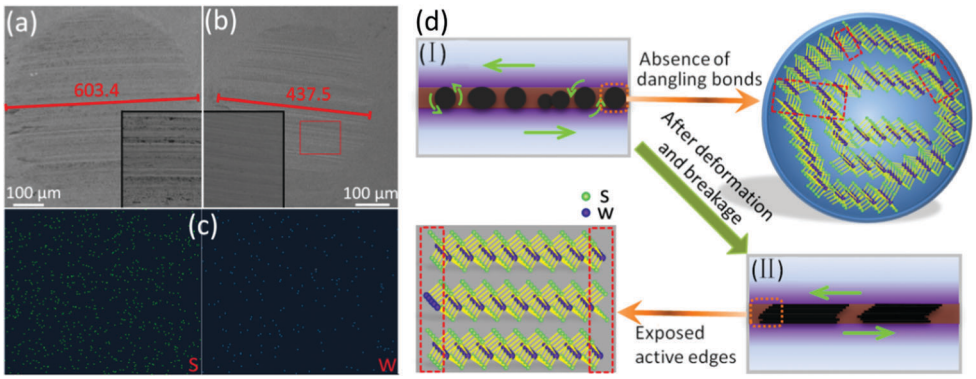


Fig. 4 (a and b) SEM images of wear scar on the testing balls lubricated by PL with 0 wt% and 1.5 wt% $WS_2$ spheres, respectively. Inset in (a and b): corresponding magnified images. (c) EDX mapping of the red quadrilateral in (b). (d) Lubricant mechanism of spherical $WS_2$ induced by LAL as additives.



spheres show more prominent reduction than those of raw slices in PL, especially at a higher temperature of 75 °C (Fig. 3). This makes the friction surface get smoother and, in consequence, helps to decrease the WSDs. On the other hand, the raw $WS_2$ slices exhibit high chemical activity as there are many chemical dangling bonds at the edge sites. So, raw $WS_2$ slices are easily oxidized to $WO_3$, which is generally considered as the main reason for the invalidation of the $WS_2$ slice lubricant because of the damage of the layered structure.[6] Due to the absence of partial dangling bonds in spherical $WS_2$, low oxidation has a positive effect during the friction process, while too high oxidation of raw $WS_2$ slices weakens the lubrication effect. Thus, the better tribological properties of smooth $WS_2$ spheres can be attributed to their ideal spherical morphology and chemical stability.

In summary, we demonstrate a novel LFR strategy to grow smooth and solid $WS_2$ submicrospheres with fewer dangling bonds. The LFR growth process includes the fragmentation of bulk-slice $WS_2$ particles and morphological reshaping by surface melting and release of surface tension energy under simple one-step laser irradiation in solution. Moreover, tribological property tests illustrate that such $WS_2$ submicrospheres dispersed in PL at an optimized concentration can effectively reduce the friction coefficient and decrease the WSD in comparison with traditional $WS_2$ slice lubricants. The excellent lubricity of spherical $WS_2$ particles is due to their rolling effect, repairing effect, and chemical stability, which all result from their smooth, solid, and spherical morphology. We expect, by this way, that the energy-loss caused by friction or wear will be reduced to a large degree and the environmental pollution induced by fossil energy consumption can be alleviated.

This work was supported by the NSFC (51472110, 11174112) and the Shandong Provincial Natural Science Foundation (JQ201214, 2014ZRB01A47, 2014ZRB01AOP). HZ acknowledges the National Basic Research Program of China (2014CB931700).

## Notes and references

1 (*a*) A. K. Geim, *Science*, 2009, **324**, 1530; (*b*) M. Xu, T. Liang, M. Shi and H. Chen, *Chem. Rev.*, 2013, **113**, 3766.
2 (*a*) Q. H. Wang, K. Kalantar-Zadeh, A. Kis, J. N. Coleman and M. S. Strano, *Nat. Nanotechnol.*, 2012, **7**, 699; (*b*) X. Huang, Z. Zeng and H. Zhang, *Chem. Soc. Rev.*, 2013, **42**, 1934.
3 (*a*) W. Li, D. Chen, F. Xia, J. Z. Tan, J. Song, W. G. Song and R. A. Caruso, *Chem. Commun.*, 2016, **52**, 4481; (*b*) K. Xu, F. Wang, Z. Wang, X. Zhan, Q. Wang, Z. Cheng, M. Safdar and J. He, *ACS Nano*, 2014, **8**, 8468.
4 (*a*) L. Joly-Pottuz, F. Dassenoy, M. Belin, B. Vacher, J. M. Martin and N. Fleischer, *Tribol. Lett.*, 2005, **18**, 477; (*b*) L. Rapoport, V. Leshchinsky, I. Lapsker, Y. Volovik, O. Nepomnyashchy, M. Lvovsky, R. Popovitz-Biro, Y. Feldman and R. Tenne, *Wear*, 2003, **255**, 785; (*c*) L. Rapoport, M. Lvovsky, I. Lapsker, W. Leshchinsky, Y. Volovik, Y. Feldman and R. Tenne, *Wear*, 2001, **249**, 149.
5 (*a*) J. C. pear, B. W. Ewers and J. D. Batteas, *Nano Today*, 2015, **10**, 301; (*b*) A. A. Alazemi, V. Etacheri, A. D. Dysart, L. E. Stacke, V. G. Pol and F. Sadeghi, *ACS Appl. Mater. Interfaces*, 2015, **7**, 5514.
6 L. Rapoport, Y. Feldman, M. Homyonfer, H. Cohen, J. Sloan, J. L. Hutchison and R. Tenne, *Wear*, 1999, **225**, 975.
7 (*a*) M. Remskar, A. Mrzel, Z. Skraba, A. Jesih, M. Ceh, J. Demsar, P. Stadelmann, F. Levy and D. Mihailovic, *Science*, 2001, **292**, 479; (*b*) R. Tenne, *Chem. – Eur. J.*, 2002, **8**, 5296; (*c*) A. Zak, Y. Feldman, V. Alperovich, R. Rosentsveig and R. Tenne, *J. Am. Chem. Soc.*, 2000, **122**, 11108; (*d*) M. Chhowalla and G. A. J. Amaratunga, *Nature*, 2000, **407**, 164; (*e*) Y. Mastai, M. Homyonfer, A. Gedanken and G. Hodes, *Adv. Mater.*, 1999, **11**, 1010; (*f*) M. Nath, A. Govindaraj and C. N. R. Rao, *Adv. Mater.*, 2001, **13**, 283.
8 (*a*) I. Wiesel, H. Arbel, A. Albu-Yaron, R. Popovitz-Biro, J. M. Gordon, D. Feuermann and R. Tenne, *Nano Res.*, 2010, **2**, 416; (*b*) N. Zink, J. Pansiot, J. Kieffer, H. A. Therese, M. Panthöfer, F. Rocker, U. Kolb and W. Tremel, *Chem. Mater.*, 2007, **19**, 6391.
9 (*a*) X. Hu, H. Gong, Y. Wang, Q. Chen, J. Zhang, S. Zheng, S. Yang and B. Cao, *J. Mater. Chem.*, 2012, **22**, 15947; (*b*) S. Yang, B. Kiraly, W. Y. Wang, S. Shang, B. Cao, H. Zeng, Y. Zhao, W. Li, Z. K. Liu, W. Cai and T. J. Huang, *Adv. Mater.*, 2012, **24**, 5598.
10 (*a*) H. Zeng, X. W. Du, S. C. Singh, S. A. Kulinich, S. Yang, J. He and W. Cai, *Adv. Funct. Mater.*, 2012, **22**, 1333; (*b*) P. Liu, W. Cai and H. Zeng, *J. Phys. Chem. C*, 2008, **112**, 3261.
11 (*a*) G. W. Yang, *Prog. Mater. Sci.*, 2007, **52**, 648; (*b*) G. W. Yang, J. Wang and Q. Liu, *J. Phys.: Condens. Matter*, 1998, **10**, 7923; (*c*) J. H. Yan, P. Liu, Z. Y. Lin, H. Wang, H. Chen, C. X. Wang and G. W. Yang, *Nat. Commun.*, 2015, **6**, 7042; (*d*) P. Liu, Y. L. Cao, C. X. Wang, X. Y. Chen and G. W. Yang, *Nano Lett.*, 2008, **8**, 2570.
12 Y. H. Chen and C. S. Yeh, *Chem. Commun.*, 2001, 371.
13 (*a*) H. Zeng, W. Cai, Y. Li, J. Hu and P. Liu, *J. Phys. Chem. B*, 2005, **109**, 18260; (*b*) P. Liu, W. Cai and H. Zeng, *J. Phys. Chem. C*, 2008, **112**, 3261; (*c*) X. Song, Z. Qiu, X. Yang, H. Gong, S. Zheng, B. Cao, H. Wang, H. Möhwald and D. Shchukin, *Chem. Mater.*, 2014, **26**, 5113; (*d*) G. Duan, X. Hu, X. Song, Z. Qiu, H. Gong and B. Cao, *Adv. Eng. Mater.*, 2015, **17**, 341.
14 (*a*) X. Zhang, X. Qiao, W. Shi, J. Wu, D. Jiang and P. Tan, *Chem. Soc. Rev.*, 2015, **44**, 2757; (*b*) A. Berkdemir, H. R. Gutiérrez, A. R. Botello-Méndez, N. Perea-López, A. L. Elías, Ch. Chia, B. Wang, V. H. Crespi, F. López-Urías, J. Charlier, H. Terrones and M. Terrones, *Sci. Rep.*, 2013, 3.
15 (*a*) A. H. Battez, J. F. Rico, A. N. Arias, J. V. Rodriguez, R. C. Rodriguez and J. D. Fernandez, *Wear*, 2006, **261**, 256; (*b*) D. Berman, A. Erdemir and A. V. Sumant, *Carbon*, 2013, **59**, 167.

 